Published in final edited form as:
Differentiation. 2009 January ; 77(1): 38–47. doi:10.1016/j.diff.2008.09.006.

AFAP120 regulates actin organization during neuronal differentiation

Xiaohua Xu[1], **Jennifer Harder**[1], **Daniel C. Flynn**[2], and **Lorene M. Lanier**[1]

1*Department of Neuroscience, University of Minnesota, Minneapolis, MN 55455*

2*Department of Microbiology & Immunology, West Virginia University, Morgantown, WV 26506.*

Abstract

During development, dynamic changes in the actin cytoskeleton determine both cell motility and morphological differentiation. In most mature tissues, cells are generally minimally motile and have morphologies specialized to their functions. In metastatic cancer, cells generally loose their specialized morphology and become motile. Therefore, proteins that regulate the transition between the motile and morphologically differentiated states can play important roles in determining cancer outcomes. AFAP120 is a neuronal specific protein that binds Src Kinase and Protein Kinase C (PKC) and cross-links actin filaments. Here we report that expression and tyrosine phosphorylation of AFAP120 are developmentally regulated in the cerebellum. In cerebellar cultures, PKC activation induces Src-kinase dependent phosphorylation of AFAP120, indicating that AFAP120 may be a downstream effector of Src. In neuroblastoma cells induced to differentiate by treatment with a PKC activator, tyrosine phosphorylation of AFAP120 appears to regulate the formation of the lamellar actin structures and subsequent neurite initiation. Together, these results indicate that AFAP120 plays a role in organizing dynamic actin structures during neuronal differentiation and suggest that AFAP120 may help regulate the transition from motile precursor to morphologically differentiated neurons.

Keywords

actin; AFAP; neuroblastoma; Src; neurite elongation

Introduction

Cell motility and morphological change are driven by dynamic reorganization of the cytoskeleton. In non-neuronal cells, cell motility is determined by dynamic polymerization and remodeling of actin filaments at the leading edge of the cell. Two distinct actin networks are involved in leading edge protrusion: lamellipodia and lamella (Ponti et al., 2004). The lamellipodium is a thin (1–3 μm) region at the edge of the cell that is important for response to chemotactic cues (DesMarais et al., 2002; Lorenz et al., 2004). The lamellum is a broader (3–10 μm) region interior to the lamellipodium. Actin dynamics in the lamellum determine the rate of motility and play an important role in cell-substrate adhesion (Gupton et al., 2005; Hotulainen and Lappalainen, 2006). In neurons after somal migration, actin based motility is largely confined to the growth cone, a dynamic structure at the tip of elongating neurites. Growth cones have an actin rich region called the transition domain that is analogous to

Address correspondence to: Lorene M. Lanier, Department of Neuroscience, 6-145 Jackson Hall, 321 Church Street SE, Minneapolis, MN 55455, tel.: 612-626-2399, fax: 612-624-7910, E-mail: lanie002@umn.edu.

lamellum; however, the growth cone periphery is dominated by filopodia and lacks well defined lamellipodia (Dent and Gertler, 2003).

Cell migration and invasion are critical in cancer cell metastasis. Neuroblastoma is the one of the most common pediatric metastatic cancer (Maris et al., 2007). The prognosis of patients with neuroblastoma is dependent on the ability of the tumor to differentiate in vivo, and treatments that induce differentiation and neurite formation reduce cell migration and invasiveness (Maris et al., 2007). In neuroblastoma tumors and cell lines, increased expression of Src kinase is associated with neurite differentiation and reduced metastatic potential (Matsunaga et al., 1998; Bjelfman et al., 1990b). Although these findings suggest that Src activity may regulate neurite differentiation, few neuronal specific downstream targets of Src have been identified.

In non-neuronal cells, the Actin Filament Associated Protein of 110kDa (AFAP110) couples activation of Src kinase and Protein kinase C (PKC) with dynamic reorganization of the actin cytoskeleton (Baisden et al., 2001b). AFAP110 was originally identified as a major substrate for tyrosine phosphorylation in Src kinase transformed fibroblasts (Flynn et al., 1992), and a point mutation in the AFAP SH3-binding domain that blocks binding to Src also inhibits tyrosine phosphorylation and association with actin, indicating that AFAP function is regulated by tyrosine phosphorylation (Baisden et al., 2001a). It is thus possible to use tyrosine phosphorylation as a biochemical readout for AFAP activity.

Alternative splicing of the AFAP gene produces isoforms of 110 and 120 kDa. While AFAP110 is expressed in most cell types, AFAP120 is specifically expressed in the nervous system (Flynn et al., 1995). AFAP110 and AFAP120 (AFAPs) are multi-domain proteins containing SH3- and SH2-binding domains, two pleckstrin homology (PH) domains, a leucine zipper and a carboxy terminal actin-binding domain (Fig. 1A). The SH3-binding domain and the amino-terminal PH1 domain interact with Src kinase and PKC, respectively (Baisden et al., 2001b). Stable complex formation with Src is regulated by the SH2-binding domains and requires Src kinase activity (Kanner et al., 1991; Reynolds et al., 1989; Guappone et al., 1998).

The leucine zipper mediates AFAP oligomerization. Tyrosine phosphorylation of AFAP regulates the state of oligomerization, shifting from higher order oligomers to smaller tetramers or dimers (Qian et al., 1998). Because AFAPs have only one filamentous actin (F-actin) binding domain, oligomerization is required for AFAPs to cross-link actin filaments (Qian et al., 1998; Qian et al., 2000). Unphosphorylated AFAP oligomers can crosslink actin filaments in vitro (Qian et al., 2000), indicating that phosphorylation is not required for F-actin binding; however, because phosphorylation regulates the size of AFAP oligomers, the amount of actin cross-linking is expected to be influenced by phosphorylation.

Studies of AFAP110 suggest that AFAPs coordinate activation of Src and PKC with dynamic actin re-organization. In non-neuronal cells, activation of PKC leads to Src activation and co-localization of Src and AFAP110 in podosomes (Qian et al., 1998; Gatesman et al., 2004). Depletion of AFAP110 blocks Src induced podosome formation (Gatesman et al., 2004) and inhibits formation of actin stress fibers and focal adhesions (Dorfleutner et al., 2007). These observations suggest that AFAP110 plays a role in the formation of actin-dependent adhesions.

Compared to AFAP110, relatively little is known about the function of the neuronal specific AFAP120. Staining of brain sections with antiserum that recognizes both AFAP110 and AFAP120 reveals that AFAPs are widely expressed in embryonic and early postnatal mouse brain regions including cortex, hippocampus, cerebellum and olfactory bulb (Clump et al., 2003). In adult brain, expression decreases and is mainly confined to regions such as the olfactory bulb that undergo continuous adult neurogenesis (Clump et al., 2003). These findings suggest that AFAPs may play a role in developing neurons. Here we report that in

differentiating neurons AFAP120 is highly expressed and tyrosine phosphorylated in a Src-dependent manner. In neuroblastoma cells, tyrosine phosphorylation of AFAP120 appears to regulate the formation of both lamellar actin structures and neurites, indicating that AFAP120 may be a downstream effector of Src during neurite differentiation.

Methods

Expression vectors and recombinant adenoviruses

Search of the mouse genome database confirmed that mouse *AFAP120* has the same intron/exon boundaries and neuronal insert (NINS) as the chicken gene. Overall, the mouse and chicken AFAP120 proteins are 86% identical. Importantly, domain structures are highly conserved (>90% amino acid identity within domains) and all the Src and PKC binding motifs and tyrosine phosphorylation sites are identical (data not shown). Therefore the chicken AFAP120 sequence was used in the current experiments. For transfection of Cos-1 cells, the cDNA encoding chicken AFAP120 and constitutively active Src527F were sub-cloned into pCMV1 as previously described for AFAP110 (Guappone et al., 1996). Tyrosine-to-phenylalanine point mutations were generated using the QuickChange kit (Stratagene). For phospho site mapping, AFAP120-8F (in which tyrosines Y93, 94, 451, 453, 531, 537, 549 and 569 mutated to phenylalanine) was used. For analysis of the role of phosphorylation in cells, AFAP120-9F (tyrosine 125 also mutated) was used because low level phosphorylation of Y125 has been detected in some systems (Guappone et al., 1998). Replication-deficient recombinant adenoviruses were produced using the pAdTrack-CMV shuttle vector and the AdEasy system (He et al., 1998). The pAdTrack-CMV shuttle vector expresses the gene of interest (e.g. AFAP120) under a CMV promoter with EGFP expressed under a second CMV promoter. EGFP expression can be monitored in live cells and used to identify infected cells and estimate expression levels. Viruses were purified on a CsCl gradient and titered on 293HEK cells as previously described (Strasser et al., 2004). Cells were infected with a multiplicity of infection (m.o.i.) of 20–40.

Immunoblot blot and phosphatase assay

Cultured cells were lysed in 50 mM Tris, 1.0% NP-40 and 150 mM NaCl containing phosphatase and protease inhibitors. Brain tissues were homogenized by sonication in lysis buffer. Protein concentration was determined using the BCA assay (Pierce). For immunoblotting, 10 μg of Cos-1 cell or cerebellar culture lysates and 40 μg of total brain/cerebellum lysates were separated on an 8% SDS-PAGE gel. For the cerebellar development blot (Fig. 2), staining of the membrane with Ponceau S after transfer was used to confirm equal loading of the lanes; it is not possible to probe with a different antiserum as a loading control because expression levels of most of the common "loading controls" (e.g. actin, tubulin, or GAPDH) change during neuronal development. For Immunoprecipitation assay, 500 μg of lysates were incubated with primary antibody at 4 °C for 1 hr and then incubated with protein-A/G beads for another 1 hr in the presence of protease and phosphatase inhibitors. For phosphatase assay, 40 μg of cerebellar neuronal lysates were mixed with 4 μg of λ-phosphatase (Upstate) and 5 mM DTT in phosphatase reaction buffer, and incubated at 37°C for 10 min. The reaction was stopped by adding 5× sample buffer and boiling for 5 min. Primary antibodies included anti-phosphotyrosine 4G10 (Upstate), anti-AFAP (Flynn et al., 1992) and anti-phospho-AFAP (PY94-AFAP; described below). For sequential probing, blots were treated with Restore Western blot stripping buffer (Pierce). Films of immunoblots were scanned and densities were measured with Photoshop software (Adobe Systems, Sa CA).

Production and analysis of phospho-AFAP antiserum

Rabbit polyclonal serum specific for phosphorylated AFAP was generated using peptide C-P-E-G-pY-pY-E-E-A-V (corresponding to amino acids 90–98 of chicken AFAPs with Y93 and

Y94 phosphorylated) as antigen. This epitope is identical in mouse and chicken AFAPs. Both tyrosines were phosphorylated because previous reports indicated that AFAP110 can be phosphorylated on both Y93 and Y94. Antisera were sequentially affinity purified using phospho- and de-phospho-peptides coupled to Sulfolink (Pierce). Testing revealed that the serum recognizes phospho-Y94 (Fig. 1); we cannot determine whether this antiserum is able to recognize phospho-Y93 because probing of the AFAP phospho-mutant blot with anti-phosphotyrosine 4G10 revealed that Y93 is not phosphorylated under these conditions (data not shown).

Dissociated Cerebellar neuronal cultures

Dissociated cerebellar cultures were prepared essentially as described (Hatten et al., 1998). Briefly, cerebella from postnatal day 3–7 (P3–P7) mice were dissected, the meninges removed and the tissue chopped into small pieces. After digestion in phosphate-buffered saline solution containing 0.125% (w/v) trypsin (Invitrogen) for 20 min at 37°C, the tissues were mechanically triturated by repeated passages through a polished Pasteur pipette in phosphatebuffered saline solution containing 0.05% (w/v) DNAse (Invitrogen). Cerebellar neurons used in biochemistry and immunocytochemistry were plated on poly-D-lysine coated dishes or coverslips, respectively, in DMEM-F12 medium (Invitrogen) containing 10% fetal calf serum and penicillin/streptomycin, and used after 1 day in vitro (DIV1). For these short term cultures, there is little glial proliferation, and it is not necessary to add mitotic inhibitors. Phorbo 12-myristate 13-acetate (PMA), bisindolylmaleimide (Bis), PP3 and PP2 were purchased from Calbiochem and used at the indicated concentrations.

Cell culture, infection and differentiation

Cos-1 cells and SH-SY5Y neuroblastoma cells were maintained in Dulbecco's modified Eagle's medium supplemented with 10% fetal calf serum and 100 unit/ml penicillin/streptomycin (Invitrogen). Cos-1 cells were plated at a density of 10^6/35-mm culture dish and allowed to grow for 12 hr before transfection using Fugene 6 reagents (Roche). Twenty-four hours after transfection, cells were lysed and subjected to immunoblotting. SH-SY5Y were induced to differentiate by addition of 16 nM PMA and culture media was changed every 24 hours for up to 3 days. For immunofluorescence, SH-SY5Y cells were plated on poly-D-lysine coated coverslips and allowed to adhere for 12–16 hours, then infected with adenovirus for 12 to 24 hours (to allow for AFAP120 expression to reach moderate levels) before being induced to differentiate by treatment with 16 nM PMA.

Immunocytochemistry and analysis

Cells were fixed for 30 min at 37°C in 4% paraformaldehyde in PHEM buffer (60 mM PIPES pH 7.0/25 mM HEPES pH 7.0/10 mM EGTA/2 mM $MgCl_2$) with 0.12M sucrose. After rinsing in PBS, coverslips were incubated in 10% fatty acid free bovine serum albumin (BSA) in PBS for 30 min, permeablized for 10 min in 0.2% triton/PBS, rinsed, and re-blocked in 10% BSA/PBS for 30 min. Alexa-labeled Phalloidin (Molecular Probes) was used to label F-actin. Primary antisera included anti-AFAP (F1) to detect AFAP110/120 (Flynn et al., 1993) and anti-Tubulin-Beta3 (Promega). Secondary antibodies were purchased from Jackson labs.

Images were acquired using a Zeiss inverted microscope with Openlab software (Improvision) and statistical analysis performed using Prism software. Analysis of the SH-SY5Y cells was done using ImageJ software. To quantitatively compare the distribution of F-actin and AFAP120 near the leading edge, the pixel intensity in each fluorescent channel was sampled along a 12 μm line. A 12μm line was used because this is generally long enough to cross from the leading edge into the interior of the cell without contacting contraction fibers at the rear of the cell. Because the purpose of this sampling was to characterize the lamellipodia and lamella domain, dorsal ruffles were omitted from sampling. Sampling was begun a few microns outside

of the cells in order to sample the background fluorescence. After subtracting background, pixel intensity was normalized such that the lowest value became 0% and the highest became 100% and the mean pixel intensity was calculated for each cell. Approximately 15–20 cells were analyzed in each treatment group. Neurites were manually traced and both primary and secondary neurites (i.e. branches) were measured. At least 75–100 cells were analyzed per treatment group.

Results

Generation of a phospho-AFAP specific antiserum

If AFAP110 and/or AFAP120 play a role in differentiating neurons, we would expect them to be expressed and tyrosine phosphorylated at the appropriate developmental stages. To facilitate this analysis, an antiserum serum specific for phosphorylated AFAPs was generated. AFAP120 is identical to AFAP110, except that AFAP120 contains an additional neuronal specific insert (NINS; Fig. 1A). AFAP110 contains 5 potential tyrosine phosphorylation sites, all of which are also found in AFAP120. In addition, the NINS exon in AFAP120 contains 4 potential tyrosine phosphorylation sites. In AFAP110, tyrosine 94 (Y94) appears to be the major phosphorylation site and Y451/453 are phosphorylated to a lesser extent (Guappone et al., 1998). Analysis of AFAP120 phospho-site mutants revealed that AFAP120 is similarly phosphorylated on Y94 and Y451/453 and is also phosphorylated on Y531/537 in the NINS (data not shown). Because Y94 is highly phosphorylated in both AFAP110 and AFAP120, we generated an antiserum specific for phospho-Y94.

To test the PY94-AFAP serum, wildtype (WT) or phospho-mutants of AFAP120 were co-expressed with activated Src (Src527F). Under these conditions, PY94-AFAP only detected a band when Y94 was not mutated (lanes containing WT or 7F-Y94, Fig. 1B, top panel). In contrast, the pan-phosphotyrosine antibody 4G10 detected robust phosphorylation of Y94 and Y451 and somewhat weaker phosphorylation of Y453 (data not shown). Together, these results indicate that the PY94-AFAP serum is specific for phosphorylated Y94. When AFAP110 or AFAP120 was co-expressed with Src527F in Cos-1 cells, PY94-AFAP and 4G10 sera detected phosphorylation of both AFAP110 and AFAP120 (Fig. 1C), indicating that PY94-AFAP serum is capable of recognizing both AFAP isoforms; however, AFAP120 appears to be relatively more phosphorylated at Y94 than AFAP110.

To test the phospho-specificity of the serum, lysates from cerebellar cultures were probed before or after treatment with lambda phosphatase. Although the cerebellar cells express both AFAP110 and AFAP120 (Fig. 1D, left panel), the PY94-AFAP antiserum only detected a band corresponding to AFAP120 (Fig. 1D, right panel; the 92 kDa band detected by PY94-AFAP in the absence of phosphatase an amino terminal proteolytic fragment of AFAP120 (Flynn et al., 1995)). Treatment with phosphatase abolished binding, indicating that the serum is phospho-specific (Fig. 1D, right panel). The fact that PY94-AFAP serum did not detect phosphorylated AFAP110 in cerebellar cultures indicates that, under these conditions, AFAP120 was more highly tyrosine phosphorylated than AFAP110. Thus, the PY94-AFAP serum specifically detects AFAP110/120 phosphorylated on tyrosine 94.

AFAP120 expression and tyrosine phosphorylation are developmentally regulated

To determine if AFAP120 and/or AFAP110 are phosphorylated, and thus activated, during periods of neuronal differentiation, mouse cerebellum lysates were probed with the PY94-AFAP serum. In the mouse cerebellum, major neuronal differentiation occurs in the first week after birth (Goldowitz and Hamre, 1998) and AFAPs are detected in the EGL, IGL and Purkinje cell layers (Clump et al., 2003). Our biochemical analysis revealed that high levels of AFAP120 expression and phosphorylation are detected during this period of cerebellar development (Fig.

2), indicating that AFAP120 may play a role in neuronal differentiation. While AFAP110 was also detected, it appeared to be expressed at lower levels and, importantly, PY94-AFAP did not detect a band at 110 kDa, suggesting that AFAP110 is not phosphorylated under these conditions. While it is formally possible that AFAP110 is phosphorylated at other tyrosine residues, immunoblot with pan phosphotyrosine antibody 4G10 did not detect a band at 110 kDa (data not shown), consistent with the conclusion that AFAP120 is the major phosphorylated isoform in the developing brain.

At P3–7, granule cell proliferation is reaching its peak (Carletti and Rossi, 2008) and granule cells are the most abundant cell type in these mixed cerebellar cultures (Hatten et al., 1998); however, it is expected that the cultures also contain other types of interneurons, Purkinje cells and some glia. At DIV1, the majority of the cultured cells are Tubulin BetaIII-positive neurons with 1–3 neurites, and AFAPs are detected in the soma, neurites and growth cone (Supplemental Fig. 1), indicating that AFAPs are present in the differentiating neurons. These data demonstrate that the peak period of AFAP120 expression and tyrosine phosphorylation correlates with the timing of neuronal differentiation and suggest that AFAP120 is the functionally important isoform in the brain. Therefore, subsequent experiments focused on the role of AFAP120.

PKC activation induces Src-dependent tyrosine phosphorylation of AFAP120

To determine if PKC regulates Src-dependent phosphorylation of AFAP120 in neurons, cerebellar cultures were treated with the PKC activator Phorbo 12-myristate 13-acetate (PMA) for 0 to 30 minutes, then lysates were immunoprecipitated with anti-AFAP serum followed by immunoblotting with PY94-AFAP serum. This analysis revealed that PKC activation induced tyrosine phosphorylation of AFAP120 that lasted for at least 30 minutes (Fig. 3A, upper panel). Significantly, phosphorylation of AFAP110 was not detected, even though AFAP110 was equally immunoprecipitated (Fig. 3A, lower panel). Treatment with the PKC specific inhibitor bisindolylmaleimide (Bis) had no significant effect on basal AFAP120 phosphorylation, but blocked PMA-induced phosphorylation (Fig. 3B), indicating that the effect of PMA is specific to activation of PKC.

To determine if PKC induced phosphorylation required Src activity, cultures were treated with PMA in the presence of the Src inhibitor PP2. Treatment with PP2 blocked PMA-induced increase in AFAP120 phosphorylation and reduced basal phosphorylation (Fig 3C, compare basal phosphorylation at time zero versus 10 min after PP2 addition). Treatment with PP3 (a structurally related compound that lacks Src inhibitory activity) had no significant effect (Fig. 3C, D). These data indicate that in differentiating neurons both basal and PKC-induced AFAP120 tyrosine phosphorylation depend on Src kinase activity.

AFAP120 localization is regulated by tyrosine phosphorylation

SH-SY5Y neuroblastoma cells were used to assess the effect of phosphorylation on AFAP120 localization. SH-SY5Y neuroblastoma can be induced to differentiate by treatment with the PKC activator PMA (Spinelli et al., 1982), and differentiation is associated with increased Src expression (Bjelfman et al., 1990a), making them useful for studying the importance of Src signaling in neuronal differentiation.

Before SH-SY5Y cell differentiation, AFAP expression levels were low (Fig. 4A), and AFAP120 tyrosine phosphorylation was virtually undetectable (Fig. 4B). After PMA treatment, expression and tyrosine phosphorylation of AFAP120 increased (Fig. 4A, B), suggesting that AFAP120 expression and phosphorylation may pay a role in SH-SY5Y differentiation.

In the first few days after SH-SY5Y cells are induced to differentiate, they are a heterogeneous mixture of cells with broad leading edges and short neurites bearing cells with actin rich growth cones; these cell morphologies are rarely seen in SH-SY5Y cells before PMA treatment (Spinelli et al., 1982). Sometimes, a single cell will have both a broad leading edge and growth cone bearing neurites (e.g. see Figure 5B). Overtime, most of the cells form neurites with actin rich growth cones, suggesting that the cells with broad leading edges represent an intermediate step in the differentiation process.

Several distinct types of actin structures were visible in SH-SY5Y cells with broad leading edges, including a lamellipodium with a loose meshwork of actin filaments, an actin rich lamella, dorsal ruffles, transverse arcs and stress fibers (Fig. 4C; for a detailed description of these actin structures, see (Ponti et al., 2004;Hotulainen and Lappalainen, 2006). In control cells, endogenous AFAPs were detected in most types of actin structures, including the lamella near the front of the cells, transverse arcs in the center of the cells and stress fibers toward the trailing ends, but AFAPs were noticeably absent from the lamellipodium at the very front of the leading edge (Fig. 4D, E).

To determine how phosphorylation affects AFAP120 localization during differentiation, recombinant adenoviruses were used to express wild type AFAP120 or non-phosphorylatable AFAP120-9F (a mutant all of the potential tyrosine phosphorylation sites were mutated to phenylalanine) in undifferentiated SH-SY5Y cells. After expression reached detectable levels (see methods), PMA was added to induce differentiation and AFAP localization was determined after 1 day of differentiation. Under these conditions, the overexpressed AFAP120-WT or AFAP120-9F will oligomerize with endogenous AFAPs and localization of the oligomers is predicted to be dependent on the properties of the overexpressed protein.

To quantitatively compare the distribution of F-actin and AFAP120 near the leading edge, the pixel intensity in each fluorescent channel was sampled along a 12μm line. This analysis revealed that all cells had a peak of F-actin staining within 10μm of the edge of the cell (red lines in graphs in Fig. 4, D–I). This peak corresponds to the lamella, which contains a meshwork of F-actin that is much more dense than the F-actin at the lamellipodium. Staining intensity for endogenous AFAPs (controls) appeared to peak just behind and partially overlap with F-actin in the lamella (green lines in Fig. 4D–E), indicating that AFAPs are associated with the interior portion of the lamella. Similar to controls, in cells expressing exogenous AFAP120-WT, AFAP staining often peaked in the interior region of the lamella and was absent from the lamellipodia (Fig. 4F). Sometimes, overexpressed AFAP120-WT sometimes appeared throughout the lamella (Fig. 4G). In contrast, in cells expressing non-phosphorylatable AFAP120-9F, AFAP120 often appeared to either be displaced toward the interior of the cell (Fig. 4H) or be completely excluded from the lamella (Fig. 4I). While we cannot conclusively prove that the AFAP120 associated with the lamella is phosphorylated (our PY-94 antiserum does not work in immunofluorescence), these data suggest that tyrosine phosphorylation of AFAP120 is required for targeting AFAP120 to the lamella. Importantly, AFAP120 associated with transverse actin arcs and stress fibers independent of its ability to be phosphorylated (Fig. 4 H–I), indicating that phosphorylation is not required for AFAP120 binding to all types of actin structures.

AFAP120 regulates the formation of dynamic F-actin structures

The previous experiments demonstrated that phosphorylated AFAP120 is specifically associated with the lamella, suggesting that AFAP120 may play a role in lamella formation. To explore this possibility, we analyzed F-actin distribution patterns in control cells and in cells overexpressing AFAP120-WT or -9F. To quantify F-actin distribution, pixel intensity was sampled along 12μm lines at 3–6 regions distributed across the leading edge of each cell. In general, the initial increase in pixel intensity in the first 1–3μm was remarkably similar in

all 6 sampling regions of an individual cell, with a rapid increase in F-actin and a peak in the center of the lamella. This initial slope in pixel intensity reflects the relative enrichment of F-actin near the periphery: the greater the amount of F-actin near the leading edge, the greater the initial slope. Pixel intensity in the interior regions of the cells reflects the relative abundance of transverse arcs and stress fibers. Each of the 6 sampling lines may encounter a different population of arcs and stress fibers, so there is more variation in intensity in the interior regions compared to regions closer to the leading edge.

Quantitative analysis revealed that cells could be put into two categories based on actin organization near the leading edge. In the first category, cells had distinct lamellipodia and lamella; in these cells F-actin levels increased gradually through the lamellipodia, peaked in the lamella within 3–5μm from the leading edge, then remained at about 50% of maximum (Fig. 5A). In the second category, cells had a broad actin rich leading edge with small or undetectable lamellipodia; in these cells, F-actin intensity rose rapidly, peaked within 1–2μm of the leading edge and then decreased to 25–35% of maximum (Fig. 5B). In controls, approximately 23% of the cells had distinct lamellipodia and lamella and 77% of cells had an actin rich leading edge (Fig. 5C). Surprisingly, all of the cells over expressing AFAP120-WT had distinct lamellipodia and lamella. Expression of AFAP120-9F shifted actin distribution slightly compared to controls, with 55% of cells having distinct lamellipodia and lamella and 45% having actin rich leading edge. These findings suggest that AFAP120 phosphorylation regulates the balance between lamellipodial and lamellar actin structures.

AFAP120 tyrosine phosphorylation alters PMA-induced neurite formation

Since AFAP120 appeared to influence actin organization (Fig 4,Fig 5), we examined the role of AFAP120 phosphorylation in neurite formation in PMA treated SH-SY5Y cells. For this analysis, a neurite was defined as a thin process at least 5 microns long with an actin rich tip (growth cone) and a length to width ratio of at least 2. Controls cells produced about 2.7 neurites per cell (Fig. 6D), with a total neurite output averaging about 83μm per cell (Fig. 6E). Compared to controls, cells over-expressing wildtype AFAP120 showed a 25% reduction in the number of neurites and a 36% reduction in total neurite output. Cells expressing non-phosphorylatable AFAP120-9F were similar to controls. The reduction in total neurite output in AFAP120-WT expressing cells was due primarily to a reduction in the number of neurites per cell (Fig 6), although a slight decrease in the length of individual neurites was detected (data not shown). These observations suggest that AFAP120 regulates neurite output in a tyrosine phosphorylation-dependent manner

Discussion

We have demonstrated that although both AFAP110 and AFAP120 are expressed in neurons, AFAP120 is relatively more abundant and more highly tyrosine phosphorylated (Fig. 1–3). Since the only difference between AFAP110 and AFAP120 is the presence of the NINS domain in AFAP120, it is likely that the NINS either provides additional Src binding sites or alters the protein conformation in a manner that enhances Src dependent phosphorylation, possibly by promoting binding to the SH2- or SH3-binding domains. Because AFAP function is regulated by tyrosine phosphorylation, these data suggest that AFAP120 is the more functionally relevant isoform in differentiating neurons.

Analysis of AFAP120 phosphorylation in cerebellar cultures (Fig. 3) and SH-SY5Y neuroblastoma cells (Fig. 4) indicated that AFAP120 is a downstream effector of PKC induced Src signaling during neuronal differentiation. In both neurons and non-neuronal cells, activation of Src and PKC induces remodeling of the actin cytoskeleton and formation of actin based adhesive structures (Mitra and Schlaepfer, 2006;Woods and Couchman, 1992;Gatlin et al., 2006;Suter and Forscher, 2001). Since AFAP120 contains an actin-binding domain, these

findings lead to the speculation that AFAP120 might regulate actin organization during neuronal differentiation.

We used SH-SY5Y neuroblastoma cells to analyze the functional importance of AFAP120 phosphorylation during neuronal differentiation. Undifferentiated SH-SY5Y neuroblastoma cells will form tumors in nude mice (Svensson et al., 2005) and their migration and invasiveness is modulated by adhesion (Meyer et al., 2004). PKC activation induces SH-SY5Y differentiation, with concomitant increased expression and tyrosine phosphorylation of AFAP120 (Fig. 4). This tyrosine phosphorylation appeared to regulate the ability of AFAP120 to associate with actin filaments in the lamella of SH-SY5Y neuroblastoma cells. In control and AFAP120-WT over expressing cells, AFAPs associate with the interior part of the lamella (Fig. 4). In cells expressing unphosphorylatable AFAP120-9F, AFAPs are found exclusively on transverse actin arcs and stress fibers, suggesting that oligomerization of endogenous AFAPs with AFAP120-9F displaces endogenous AFAPs from the lamella. Intriguingly, even though its localization was similar to that of endogenous AFAPs, over expression of AFAP120-WT dramatically altered actin distribution patterns (Fig. 5); all of the AFAP120-WT cells had distinct lamellipodia and lamella, while the majority of the control cells had actin rich leading edges and small or undetectable lamellipodia. In cells expressing AFAP120-9F, the more completely AFAPs were excluded from the leading edge, the more dramatic was the leading edge actin enrichment (compare Fig. 4H and I). Together, these observations suggest a model in which phosphorylated AFAP120 helps to establish distinct lamella and lamellipodia.

There is precedence for changes in the level of individual actin binding proteins altering the balance between lamella and lamellipodia (Iwasa and Mullins, 2007; Gupton et al., 2005; Ponti et al., 2004; Blanchoin et al., 2001). Combined with our data, this suggests a model in which cross-linking of actin filaments by phospho-AFAP120 regulates activity of other actinbinding protein(s), leading to the formation of distinct lamella and lamellipodia. In this model, removal of AFAP120 from the lamella (by over expression of AFAP120-9F or by reducing levels of endogenous phosphorylation), alters activity of other actin regulatory proteins, leading to formation of an actin rich leading edge. Compatible with this model, increased levels of unphosphorylated AFAP120 on transverse actin arcs and stress fibers may affect the ability of other proteins to expand the lamella, increasing the percent of cells with distinct lamella and lamellipodia.

It is important to note that the lamella and lamellipodia are technically defined by their orientation to each other and the rates of actin polymerization and turnover, not by the density of actin per se (Ponti et al., 2004). For that reason we do not refer to the expanded actin rich region in control and AFAP120-9F expressing cells as "lamella"; it would be necessary to monitor the dynamics of actin turnover to determine if it is a bona fide lamella. In some reports, the actin rich leading edges seen during SH-SY5Y differentiation have been called growth cones (Kim and Feldman, 1998). While the term growth cone typically refers to an actin rich structure at the tip of a thin, microtubule rich neurite, it seems likely that the SH-SY5Y cells with actin rich leading edges represent an intermediate step in neurite differentiation. In this context, the level of phosphorylatable AFAP120 may affect growth cone formation and neurite initiation. Before neuronal precursor cells are fully morphologically differentiated, such as the case with SH-SY5Y cells, high levels of phosphorylated AFAP120 favor formation of distinct lamellipodia and lamella and may block neurite initiation. However, given the relatively high levels of AFAP120 expressed in the developing cerebellum and in cultured neurons at a time when neurites are rapidly elongating, it seems likely that AFAP120 also plays a role in growth cone migration and axon elongation.

Our data reveal a correlation between increased expression and tyrosine phosphorylation of AFAP120 and neuronal differentiation. Supporting our findings, others have demonstrated that

increased levels of Src correlate with neuroblastoma differentiation and improved patient prognosis (Matsunaga et al., 1994) and that increased levels of AFAPs correlate with reduced relapse and recurrence of human neuroblastomas (Rhodes et al., 2004). In contrast, high levels of AFAP110 are associated with increased adhesion and growth in breast and prostate cancer cells (Walker et al., 2007; Zhang et al., 2007). These findings suggest that AFAP120 and AFAP110 may play fundamentally different roles in tumor cells. Increased expression of AFAP110 enhances growth and motility in non-neuronal cells, while increased expression of AFAP120 correlate with reduced proliferation and differentiation in neuronal cells. Whether these differences reflect different functions of AFAP110 and AFAP120 in actin remodeling and adhesion remains to be determined.

Supplementary Material

Refer to Web version on PubMed Central for supplementary material.

Acknowledgements

We would like to thank Paul Letourneau, Frank Gertler, Meg Titus, Lihsia Chen, Maria Morabito and Paul Mermelstein for critical reading of this manuscript. This research was supported by NIH RO1NS049178 and Academic Health Center Seed Grant 2003–39 to L.M.L.

References

Baisden JM, Gatesman AS, Cherezova L, Jiang BH, Flynn DC. The intrinsic ability of AFAP-110 to alter actin filament integrity is linked with its ability to also activate cellular tyrosine kinases. Oncogene 2001a;20:6607–6616. [PubMed: 11641786]

Baisden JM, Qian Y, Zot HM, Flynn DC. The actin filament-associated protein AFAP-110 is an adaptor protein that modulates changes in actin filament integrity. Oncogene 2001b;20:6435–6447. [PubMed: 11607843]

Bjelfman C, Meyerson G, Cartwright CA, Mellstrom K, Hammerling U, Pahlman S. Early activation of endogenous pp60src kinase activity during neuronal differentiation of cultured human neuroblastoma cells. Molecular & Cellular Biology 1990a;10:361–370. [PubMed: 2136766]

Bjelfman C, Meyerson G, Cartwright CA, Mellstrom K, Hammerling U, Pahlman S. Early activation of endogenous pp60src kinase activity during neuronal differentiation of cultured human neuroblastoma cells. Mol Cell Biol 1990b;10:361–370. [PubMed: 2136766]

Blanchoin L, Pollard TD, Hitchcock-DeGregori SE. Inhibition of the Arp2/3 complex-nucleated actin polymerization and branch formation by tropomyosin. Curr Biol 2001;11:1300–1304. [PubMed: 11525747]

Carletti B, Rossi F. Neurogenesis in the cerebellum. Neuroscientist 2008;14:91–100. [PubMed: 17911211]

Clump DA, Clem R, Qian Y, Guappone-Koay A, Berrebi AS, Flynn DC. Protein expression levels of the Src activating protein AFAP are developmentally regulated in brain. J Neurobiol 2003;54:473–485. [PubMed: 12532398]

Dent EW, Gertler FB. Cytoskeletal dynamics and transport in growth cone motility and axon guidance. Neuron 2003;41:209–227. [PubMed: 14556705]

DesMarais V, Ichetovkin I, Condeelis J, Hitchcock-DeGregori SE. Spatial regulation of actin dynamics: a tropomyosin-free, actin-rich compartment at the leading edge. J Cell Sci 2002;115:4649–4660. [PubMed: 12415009]

Dorfleutner A, Stehlik C, Zhang J, Gallick GE, Flynn DC. AFAP-110 is required for actin stress fiber formation and cell adhesion in MDA-MB-231 breast cancer cells. Journal of cellular physiology 2007;213:740–749. [PubMed: 17520695]

Flynn DC, Koay TC, Humphries CG, Guappone AC. AFAP-120. A variant form of the Src SH2/SH3-binding partner AFAP-110 is detected in brain and contains a novel internal sequence which binds to a 67-kDa protein. J Biol Chem 1995;270:3894–3899. [PubMed: 7876134]

Flynn DC, Schaller MD, Parsons JT. Tyrosine phosphorylation of a 120,000 dalton membrane-associated protein by the neural form of pp60c-src, pp60c-src+ Oncogene 1992;7:579–583. [PubMed: 1372401]

Gatesman A, Walker VG, Baisden JM, Weed SA, Flynn DC. Protein kinase Calpha activates c-Src and induces podosome formation via AFAP-110. Mol Cell Biol 2004;24:7578–7597. [PubMed: 15314167]

Gatlin JC, Estrada-Bernal A, Sanford SD, Pfenninger KH. Myristoylated, alanine-rich C-kinase substrate phosphorylation regulates growth cone adhesion and pathfinding. Mol Biol Cell 2006;17:5115–5130. [PubMed: 16987960]

Goldowitz D, Hamre K. The cells and molecules that make a cerebellum. Trends Neurosci 1998;21:375–382. [PubMed: 9735945]

Guappone AC, Weimer T, Flynn DC. Formation of a stable src-AFAP-110 complex through either an amino-terminal or a carboxy-terminal SH2-binding motif. Mol Carcinog 1998;22:110–119. [PubMed: 9655255]

Gupton SL, Anderson KL, Kole TP, Fischer RS, Ponti A, Hitchcock-DeGregori SE, Danuser G, Fowler VM, Wirtz D, Hanein D, Waterman-Storer CM. Cell migration without a lamellipodium: translation of actin dynamics into cell movement mediated by tropomyosin. J Cell Biol 2005;168:619–631. [PubMed: 15716379]

Hatten, ME.; Gao, W-Q.; Morrison, ME.; Fischer, RS. The cerebellum: purification and co-culture of identified cell populations. In: Banker, G.; G, K., editors. Culturing Nerve Cells. Cambridge, MA: MIT Press; 1998. p. 419-459.

Hotulainen P, Lappalainen P. Stress fibers are generated by two distinct actin assembly mechanisms in motile cells. J Cell Biol 2006;173:383–394. [PubMed: 16651381]

Iwasa JH, Mullins RD. Spatial and temporal relationships between actin-filament nucleation, capping, and disassembly. Curr Biol 2007;17:395–406. [PubMed: 17331727]

Kanner SB, Reynolds AB, Wang HC, Vines RR, Parsons JT. The SH2 and SH3 domains of pp60src direct stable association with tyrosine phosphorylated proteins p130 and p110. Embo J 1991;10:1689–1698. [PubMed: 1710979]

Kim B, Feldman EL. Differential regulation of focal adhesion kinase and mitogen-activated protein kinase tyrosine phosphorylation during insulin-like growth factor-I-mediated cytoskeletal reorganization. J Neurochem 1998;71:1333–1336. [PubMed: 9721762]

Lorenz M, DesMarais V, Macaluso F, Singer RH, Condeelis J. Measurement of barbed ends, actin polymerization, and motility in live carcinoma cells after growth factor stimulation. Cell Motil Cytoskeleton 2004;57:207–217. [PubMed: 14752805]

Maris JM, Hogarty MD, Bagatell R, Cohn SL. Neuroblastoma. Lancet 2007;369:2106–2120. [PubMed: 17586306]

Matsunaga T, Shirasawa H, Enomoto H, Yoshida H, Iwai J, Tanabe M, Kawamura K, Etoh T, Ohnuma N. Neuronal src and trk a protooncogene expression in neuroblastomas and patient prognosis. International journal of cancer 1998;79:226–231.

Matsunaga T, Shirasawa H, Tanabe M, Ohnuma N, Kawamura K, Etoh T, Takahashi H, Simizu B. Expression of neuronal src mRNA as a favorable marker and inverse correlation to N-myc gene amplification in human neuroblastomas. International journal of cancer 1994;58:793–798.

Meyer A, van Golen CM, Kim B, van Golen KL, Feldman EL. Integrin expression regulates neuroblastoma attachment and migration. Neoplasia (New York, N.Y 2004;6:332–342.

Mitra SK, Schlaepfer DD. Integrin-regulated FAK-Src signaling in normal and cancer cells. Curr Opin Cell Biol 2006;18:516–523. [PubMed: 16919435]

Ponti A, Machacek M, Gupton SL, Waterman-Storer CM, Danuser G. Two distinct actin networks drive the protrusion of migrating cells. Science 2004;305:1782–1786. [PubMed: 15375270]

Qian Y, Baisden JM, Westin EH, Guappone AC, Koay TC, Flynn DC. Src can regulate carboxy terminal interactions with AFAP-110, which influence self-association, cell localization and actin filament integrity. Oncogene 1998;16:2185–2195. [PubMed: 9619827]

Qian Y, Baisden JM, Zot HG, Van Winkle WB, Flynn DC. The carboxy terminus of AFAP-110 modulates direct interactions with actin filaments and regulates its ability to alter actin filament integrity and induce lamellipodia formation. Exp Cell Res 2000;255:102–113. [PubMed: 10666339]

Reynolds AB, Kanner SB, Wang HC, Parsons JT. Stable association of activated pp60src with two tyrosine-phosphorylated cellular proteins. Mol Cell Biol 1989;9:3951–3958. [PubMed: 2476666]

Rhodes DR, Yu J, Shanker K, Deshpande N, Varambally R, Ghosh D, Barrette T, Pandey A, Chinnaiyan AM. ONCOMINE: a cancer microarray database and integrated data-mining platform. Neoplasia (New York, N.Y 2004;6:1–6.

Spinelli W, Sonnenfeld KH, Ishii DN. Effects of phorbol ester tumor promoters and nerve growth factor on neurite outgrowth in cultured human neuroblastoma cells. Cancer Res 1982;42:5067–5073. [PubMed: 7139611]

Suter DM, Forscher P. Transmission of growth cone traction force through apCAM-cytoskeletal linkages is regulated by Src family tyrosine kinase activity. J Cell Biol 2001;155:427–438. [PubMed: 11673478]

Svensson A, Azarbayjani F, Backman U, Matsumoto T, Christofferson R. Digoxin inhibits neuroblastoma tumor growth in mice. Anticancer research 2005;25:207–212. [PubMed: 15816540]

Walker VG, Ammer A, Cao Z, Clump AC, Jiang BH, Kelley LC, Weed SA, Zot H, Flynn DC. PI3K activation is required for PMA-directed activation of cSrc by AFAP-110. Am J Physiol Cell Physiol 2007;293:C119–C132. [PubMed: 17360811]

Woods A, Couchman JR. Protein kinase C involvement in focal adhesion formation. J Cell Sci 1992;101 (Pt 2):277–290. [PubMed: 1629245]

Zhang J, Park SI, Artime MC, Summy JM, Shah AN, Bomser JA, Dorfleutner A, Flynn DC, Gallick GE. AFAP-110 is overexpressed in prostate cancer and contributes to tumorigenic growth by regulating focal contacts. The Journal of clinical investigation 2007;117:2962–2973. [PubMed: 17885682]

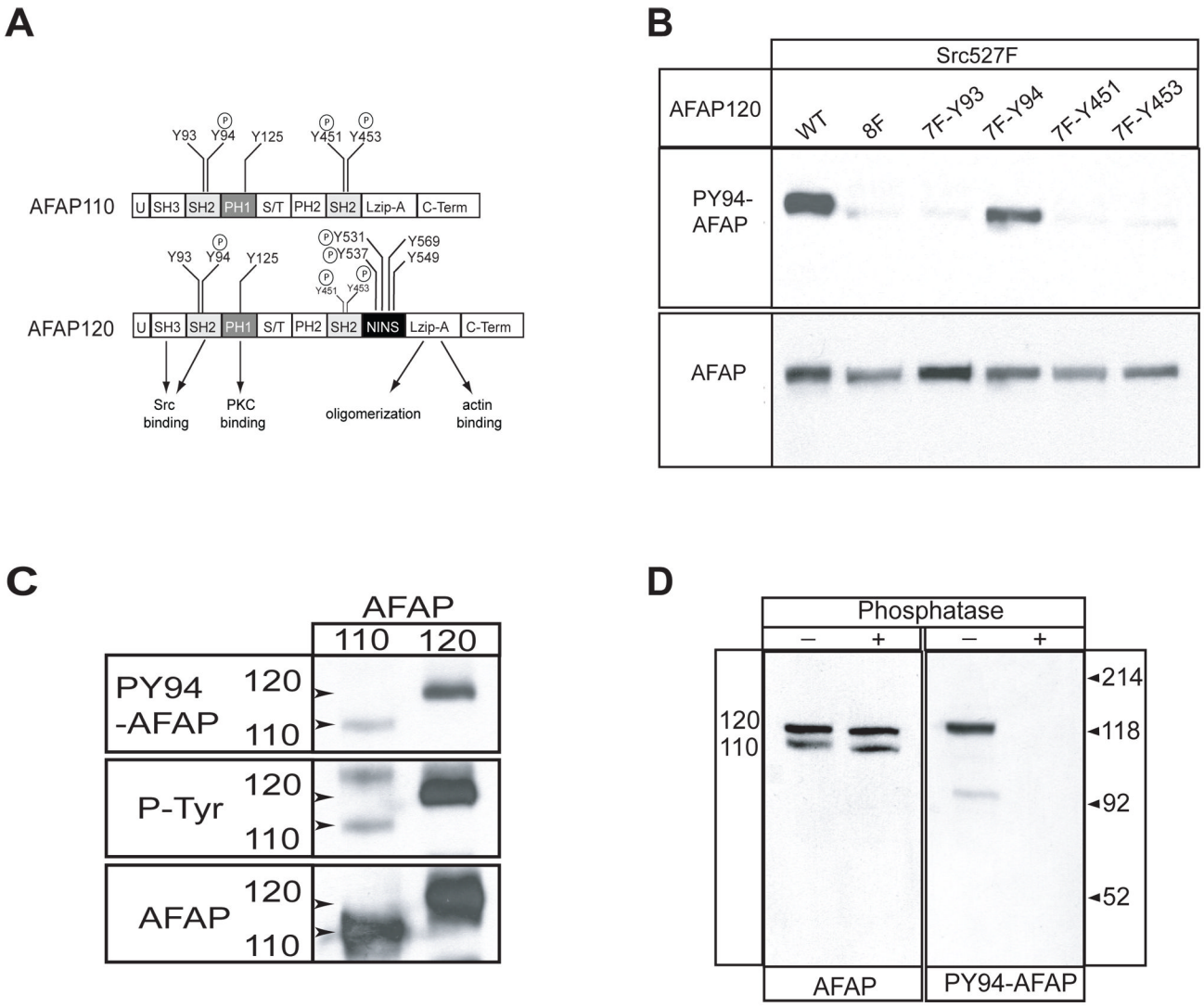

Figure 1. Characterization of PY94-AFAP, a phospho-epitope specific antiserum against phosphorylated AFAP110/120 Tyrosine-94

(A) Schematic map of AFAP110 and AFAP120 in which the positions of the tyrosine residues are indicated. AFAP110 and AFAP120 proteins contain identical SH3- and SH2-binding domains, two pleckstrin homology domains (PH1 and PH2), a serine/threonine rich region (S/T) and a leucine zipper motif within which lies an actin-binding domain (Lzip-A). AFAP120 contains a Neuronal Insert (NINS), generated by alternative splicing. Positions of the phosphorylated tyrosines are indicated by an encircle 'P'. (B) The PY94-AFAP antiserum was used to probe a western blot of wildtype and phospho-mutant AFAP120, including 120-8F (tyrosines Y93, 94, 451, 453, 531, 537, 549 and 569 mutated to phenylalanine) and 120-7F-Y93/94/451/453, in which 7 tyrosines are mutated and only the indicated tyrosine (Y93, 94, 451 or 453) remained. The indicated cDNA was transfected into Cos-1 cells with autoactive Src kinase (Src527F). Immunoblots of the cell lysates were sequentially probed with antisera PY94-AFAP and anti-AFAP. (C) Immunoblot of Cos-cells expressing AFAP110 or AFAP120 sequentially probed with antisera PY94-AFAP, total AFAP (F1) and 4G10 pan-phosphotyrosine (P-Try). (D) Phospho-specificity of the PY94-AFAP serum was demonstrated

by treating cerebellar culture lysates with (+) or without (−) λ-phosphatase, then immunoblotting and sequentially probing with PY94-AFAP and total AFAP antisera.

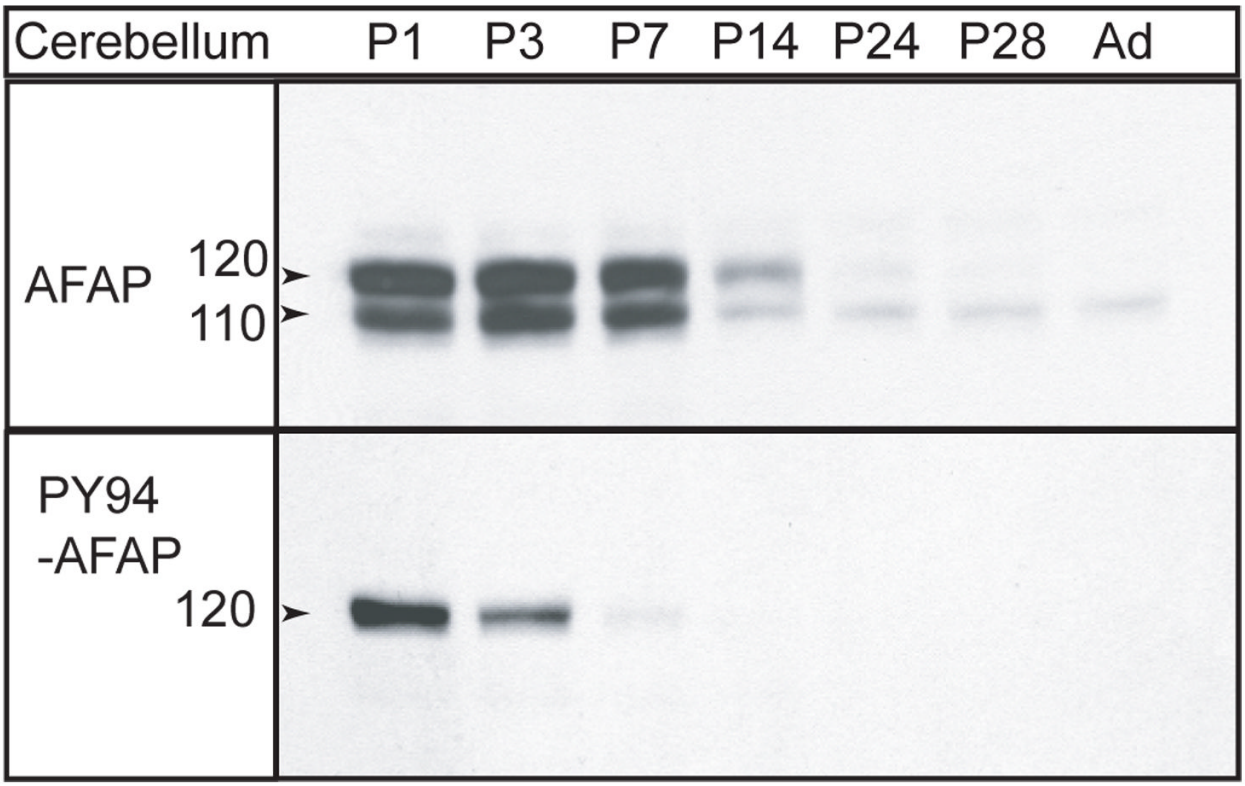

Figure 2. AFAP110/120 expression and tyrosine phosphorylation in the developing cerebellum

Immunoblot analysis of lysates prepared from postnatal day 1 through 28 (P1 to P28) and adult (Ad) mouse cerebella. The blot was sequentially probed with PY94-AFAP and total AFAP (F1) antisera. The positions of AFAP110 and AFAP120 are indicated on the left.

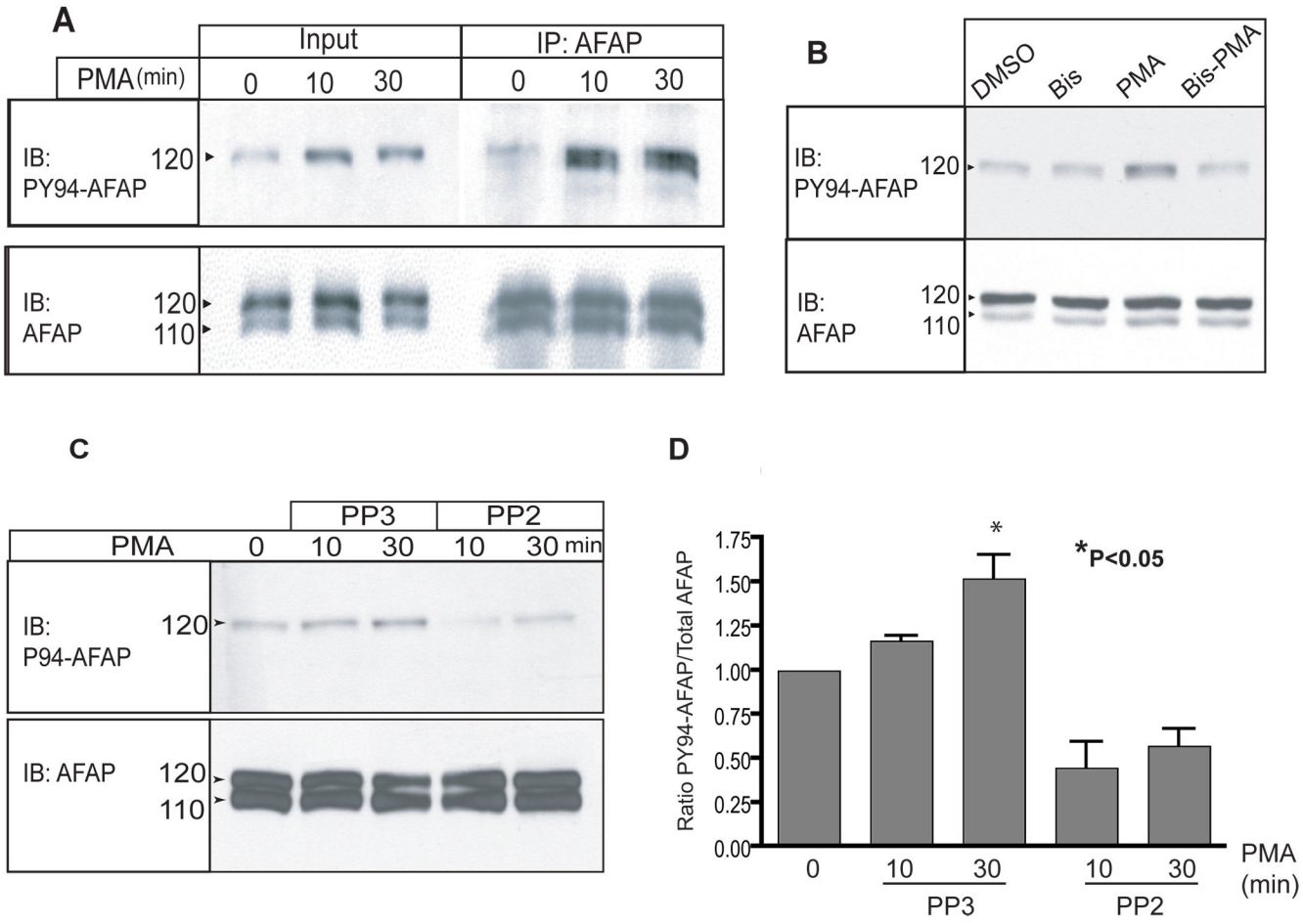

Figure 3. PKC-induces Src kinase-dependant tyrosine phosphorylation of AFAP in cerebellar cultures

Cerebellar cultures were treated with the indicated compound(s) and the cell lysates were sequentially immunoblotted (IB) with antisera against PY94-AFAP and total AFAP. (A) Time course of treatment with 100 nM PMA. The left panel shows total protein input, the right panel immunoprecipitation (IP) with anti-AFAP. (B) Cultures were treated for 30 min. with DMSO, 100 nM BIS, PMA alone or PMA with BIS. (C) Cultures were treated for the indicated time with 100 nM PMA in the presence of 1 μM PP3 or PP2. (D) Quantification of the results in (C), normalized to the untreated lysates (time 0, left most lane) and presented as the ratio of PY94-AFAP/total AFAP, mean ± S.E.M.

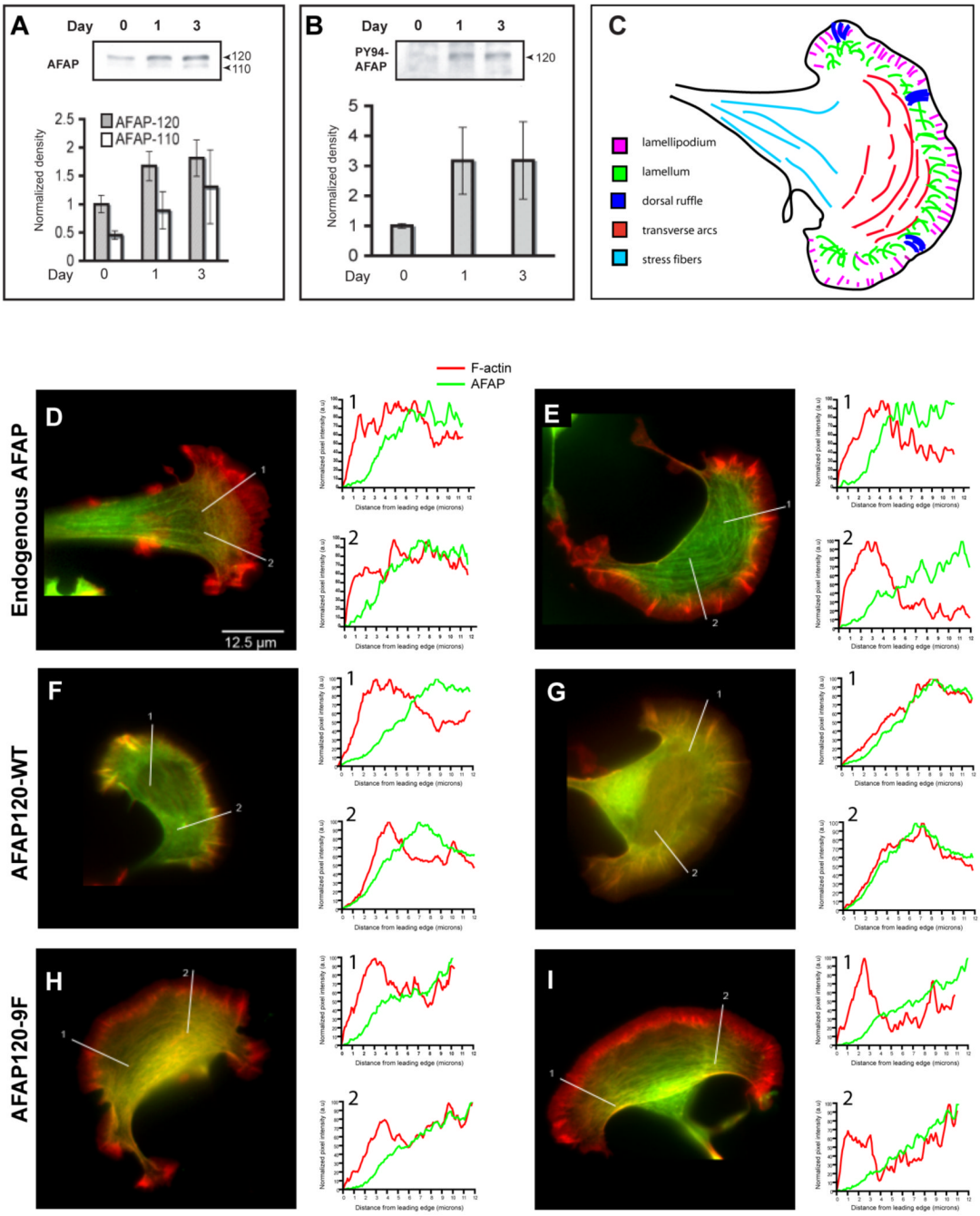

Figure 4. AFAP120 localization is regulated by tyrosine phosphorylation

(A–B) Immunoblots of SH-SY5Y neuroblastoma cells treated with 16 nM PMA for 1–3 days to induce differentiation. To detect endogenous AFAPs, blots were sequentially probed with antisera to total AFAP (A) and PY94-AFAP (B). n= 3 western blots. Error bars are ±S.E.M. (C) Diagram illustrating the organization of a F-actin structures in a typical cell with a broad leading edge: lamellipodium (pink), lamellum (green), dorsal ruffles (dark blue), transverse arcs (red) and stress fibers (light blue). Differentiating SH-SY5Y cells expressing (D–E) endogenous AFAPs, (F–G) AFAP120-WT, or (H–I) AFAP120-9F were fixed and stained with anti-AFAP (green) and phalloidin to detect F-actin (red). Co-localization of AFAP and F-actin appears yellow. Graphs are plots of pixel intensity (arbitrary units) versus distance from the

edge of the cell for the AFAP (green line) and F-actin (red line) staining measured along the 12 μm lines shown in the corresponding merged image panels.

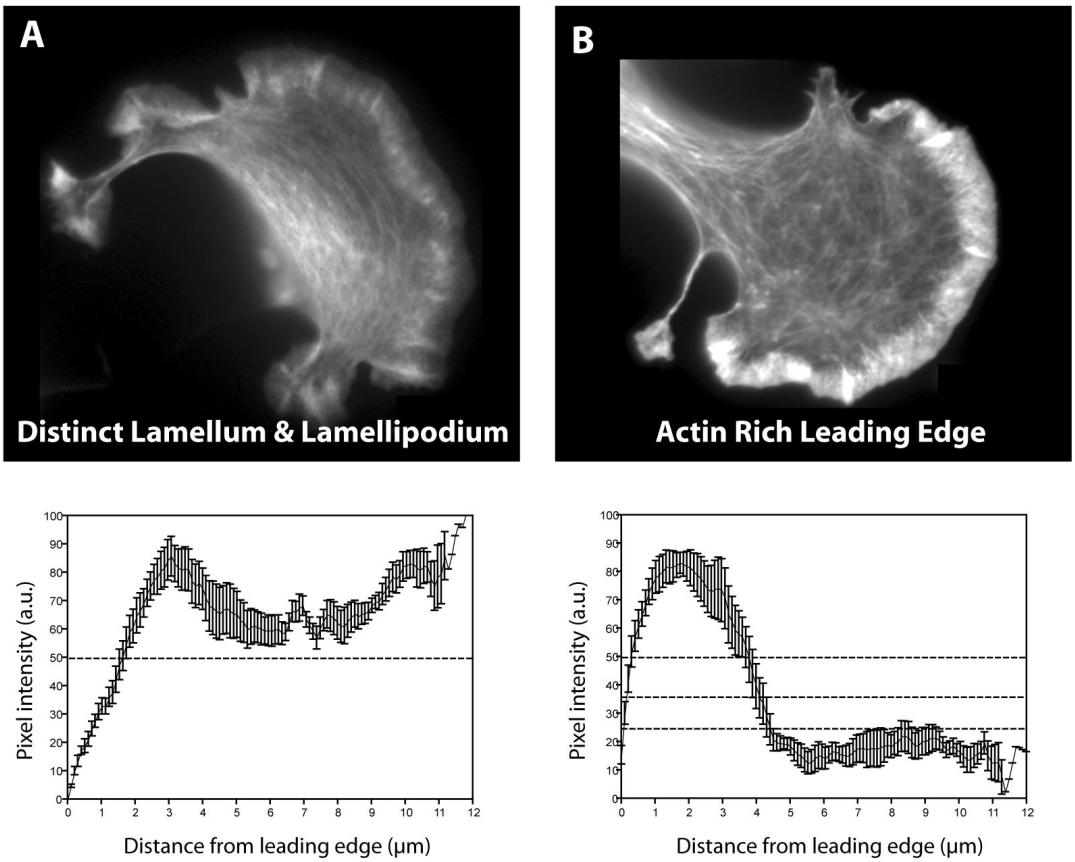

C

Percentage of Cells in each F-actin Distrubution Category

Cells expressing:	Distinct Lamella & Lamellipodia	Actin Rich Leading Edge
control	23%	77%
AFAP120-WT	100%	0%
AFAP120-9F	55%	45%

Figure 5. AFAP120 regulates F-actin distribution in differentiating SH-SY5Y neuroblastoma cells

F-actin pixel intensity was sampled across the leading edge of control SH-SY5Y cells and in cells over expressing either AFAP120-WT or AFAP120-9F and the mean normalized pixel intensity plotted versus distance from the leading edge. F-actin staining and intensity plots are shown for representative cells. Based on the intensity plots, cells could be characterized as either (A) having distinct lamella and lamellipodia or (B) having an actin rich leading edge. (C) Table summarizing the percentage of cells with each F-actin distribution pattern.

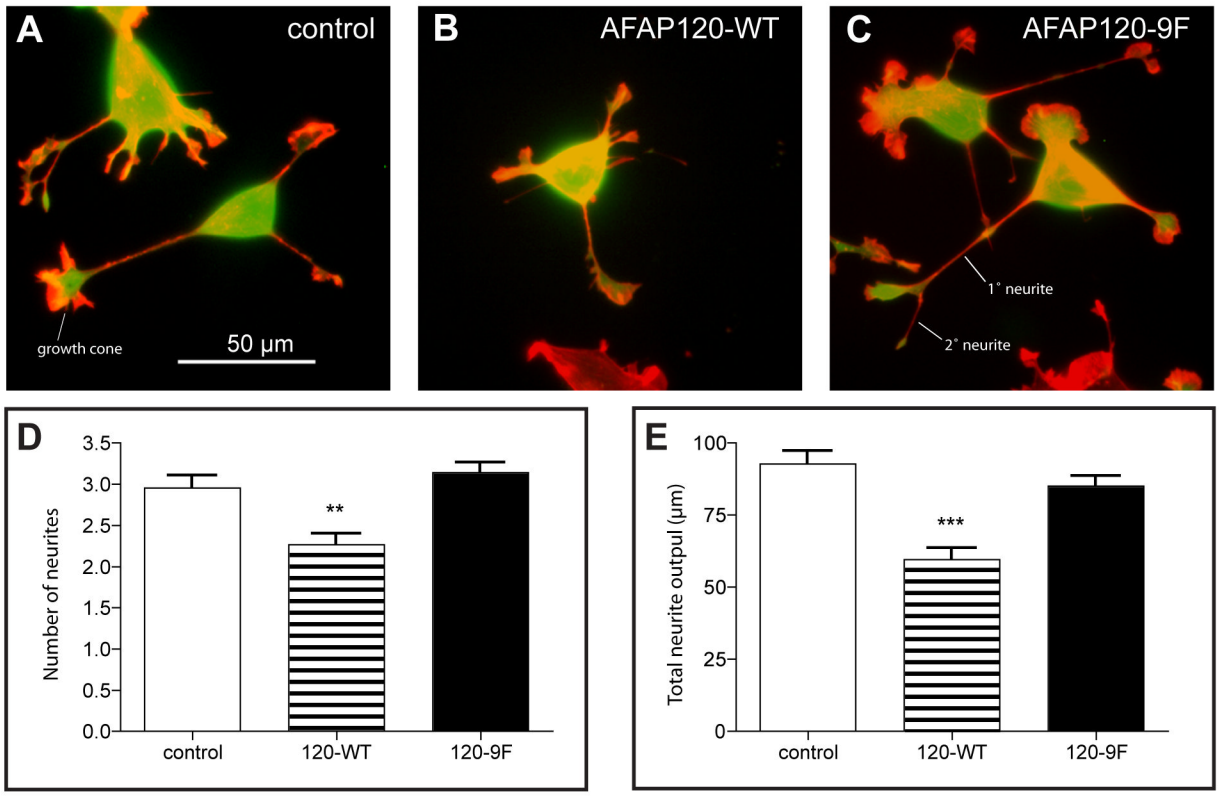

Figure 6. AFAP120 alters SH-SY5Y neurite elongation in a tyrosine-phosphorylation-dependent manner

Immunofluorescence of differentiating SH-SY5Y cells expressing (**A**) EGFP alone (control), or EGFP co-expressed with (**B**) AFAP120-WT (wildtype) or (**C**) phospho-mutant AFAP120-9F, then fixed and stained with to show F-actin (red) and EGFP (green). Quantification of the number of (**D**) neurites per cell and (E) total neurite output. Significance was determined by one way ANOVA with Bonferroni post hoc analysis and values are shown as mean±S.E. AFAP120-WT is significantly different (**=P<0.05, ***=P<0.001) from control and AFAP120-9F.